Environment International 133 (2019) 105138

Contents lists available at ScienceDirect

Environment International

journal homepage: www.elsevier.com/locate/envint

New insights into organ-specific oxidative stress mechanisms using a novel biosensor zebrafish

Sulayman Mourabit*, Jennifer A. Fitzgerald, Robert P. Ellis, Aya Takesono, Cosima S. Porteus, Maciej Trznadel, Jeremy Metz, Matthew J. Winter, Tetsuhiro Kudoh, Charles R. Tyler*

Biosciences, College of Life and Environmental Sciences, University of Exeter, UK

ARTICLE INFO

Handling Editor: Adrian Covaci

Keywords:
Oxidative stress
Zebrafish
Toxicants
Biosensor

ABSTRACT

Background: Reactive oxygen species (ROS) arise as a result from, and are essential in, numerous cellular processes. ROS, however, are highly reactive and if left unneutralised by endogenous antioxidant systems, can result in extensive cellular damage and/or pathogenesis. In addition, exposure to a wide range of environmental stressors can also result in surplus ROS production leading to oxidative stress (OS) and downstream tissue toxicity.

Objectives: Our aim was to produce a stable transgenic zebrafish line, unrestricted by tissue-specific gene regulation, which was capable of providing a whole organismal, real-time read-out of tissue-specific OS following exposure to a wide range of OS-inducing environmental contaminants and conditions. This model could, therefore, serve as a sensitive and specific mechanistic *in vivo* biomarker for all environmental conditions that result in OS.

Methods: To achieve this aim, we exploited the pivotal role of the electrophile response element (EpRE) as a globally-acting master regulator of the cellular response to OS. To test tissue specificity and quantitative capacity, we selected a range of chemical contaminants known to induce OS in specific organs or tissues, and assessed dose-responsiveness in each using microscopic measures of mCherry fluorescence intensity.

Results: We produced the first stable transgenic zebrafish line Tg (*3EpRE:hsp70:mCherry*) with high sensitivity for the detection of cellular RedOx imbalances, *in vivo* in near-real time. We applied this new model to quantify OS after exposure to a range of environmental conditions with high resolution and provided quantification both of compound- and tissue-specific ROS-induced toxicity.

Discussion: Our model has an extremely diverse range of potential applications not only for biomonitoring of toxicants in aqueous environments, but also in biomedicine for identifying ROS-mediated mechanisms involved in the progression of a number of important human diseases, including cancer.

1. Introduction

Reactive oxygen species (ROS) can result from numerous metabolic processes that occur in all aerobic organisms, and have essential physiological roles, for example, in cell signalling, immunity and apoptosis (Forman and Torres, 2002; Burhans and Heintz, 2009; Ray et al., 2012; Kehrer and Klotz, 2015). ROS, however, are highly reactive and unneutralised can induce damage to intracellular lipids, proteins, RNA, and DNA (Freeman and Crapo, 1982). Consequently, cellular RedOx homeostasis is maintained through an intricate balance of ROS production and neutralisation by endogenous antioxidant systems. Exposure to virtually any stressor can result in surplus ROS production causing a change in cellular RedOx status in a process termed oxidative stress (OS) (Lushchak, 2011). In the case of exogenous chemical toxicants taken up into cells, the production of free radicals can result as a consequence of phase I metabolism via the cytochrome P450 system or via mitochondria (Liska, 1998). Importantly, sustained oxidative stress can lead to the chronic inflammation, associated with many human diseases including cancer, diabetes, dementia, and cardiovascular disorders (Faria and Persaud, 2017; Maritim et al., 2003; Poprac et al., 2017; Wiegman et al., 2015). Furthermore, the inflammatory pathway stimulates the production of free radicals, thereby creating a feedback loop of oxidative stress.

A crucial cellular mechanism for maintaining RedOx homeostasis is

* Corresponding authors at: Biosciences, College of Life and Environmental Sciences, Geoffrey Pope Building, University of Exeter, Exeter, Devon EX4 4QD, UK (C.R. Tyler). School of Life Sciences and Facility Management, Campus Grüental, Zurich University of Applied Sciences, Wädenswil 8820, Switzerland (S. Mourabit).
E-mail addresses: sulayman.mourabit@zhaw.ch (S. Mourabit), c.r.tyler@exeter.ac.uk (C.R. Tyler).

https://doi.org/10.1016/j.envint.2019.105138
Received 31 May 2019; Received in revised form 8 August 2019; Accepted 27 August 2019
Available online 20 October 2019

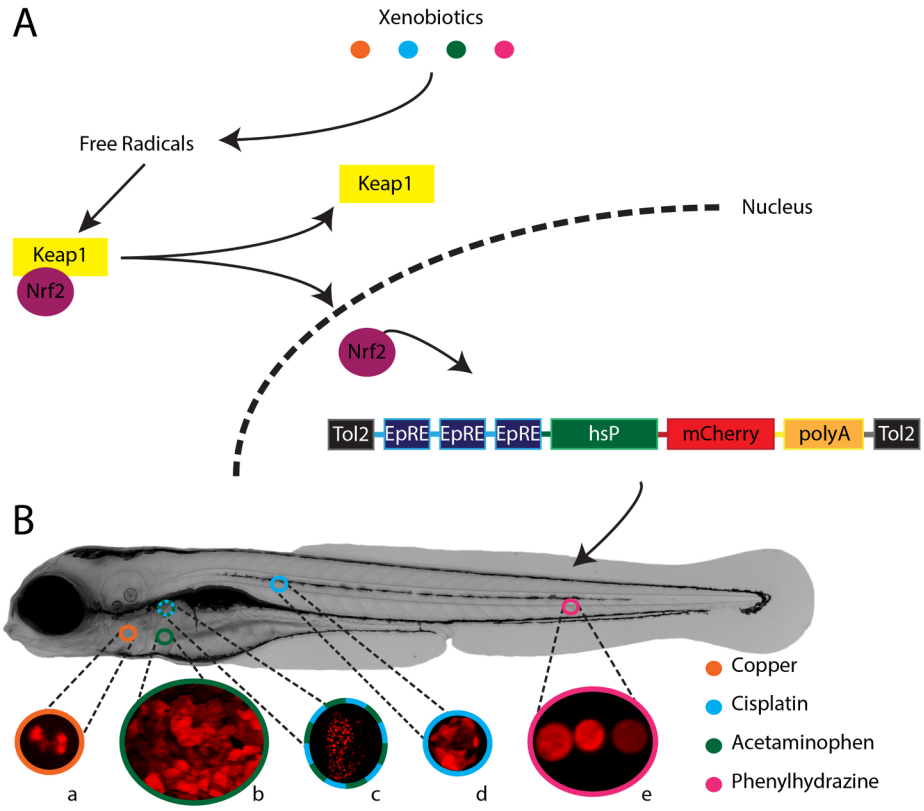

Fig. 1. Chemical-dependent tissue-specific responses in the zebrafish transgenic EpRE line Tg (3EpRE:hsp70:mCherry). (A) Simplified overview of the Keap1-Nrf2 pathway and activation of the 3EpRE:hsp70:mCherry transgene. (B): Compounds tested and their target tissues are represented by the coloured circles on a 4 day old zebrafish larva. Enlarged circles display a, ionocytes; b, hepatocytes; c, pronephric proximal tubules; d, neuromasts; e, erythrocytes.

the Nrf2 transcription factor (Nrf2-Keap1 regulatory system). This pathway oversees the regulation of hundreds of cytoprotective genes by acting on the Electrophile Response Element (EpRE), otherwise known as the Antioxidant Response Element (ARE), which in turn mediates the induction of phase II detoxifying enzymes and metabolic responses to oxidative stress (Itoh et al., 2010; Kobayashi and Yamamoto, 2006; Nakajima et al., 2011). Notwithstanding its protective effects, excessive activation of the Nrf2 pathway will reduce apoptosis and create favourable conditions for normal, as well as malignant, cells by protecting them not only against oxidative stress, but also chemotherapeutic agents (Menegon et al., 2016). Consequently, this regulatory system plays a key role in the progression and persistence of many human cancers. The Nrf2-Keap1 system is highly conserved among vertebrates, and tissue-restricted induction appears to be an intrinsic feature of Nrf2 target genes across multiple species (Nakajima et al., 2011; Kobayashi et al., 2002). For example, microarray analysis has revealed that the Nrf2 transcription factor is critical in regulating genes in the OS pathway in zebrafish embryos (Nakajima et al., 2011). All vertebrate glutathione–S-transferase (GST) genes that encode for members of a family of protein catalysing the conjugation of glutathione to electrophiles also possess an EpRE-like sequence in the regulatory region necessary for Nrf2-activated transcription (Suzuki et al., 2005; Tsujita et al., 2011).

To date, studies into the modulation of the Nrf2-Keap1 system have focused on target genes and downstream protective pathway components. However, OS analyses conducted using Nrf2 target genes, such as *gstp1*, or whole-mount *in situ* hybridisation targeting genes including *gstp1*, *hmox1a*, or *fthl*, are limited to those tissues that express these individual genes, whereas xenobiotic agents may activate Nrf2 across the whole organism (Nakajima et al., 2011; Tsujita et al., 2011). Numerous genes, therefore, have to be tested to identify the toxicity profile of one chemical, increasing the effort required to analyse the cellular ReDox profile of each compound. Transgenic lines exploiting ROS-scavenging proteins developed to date, such as Hyper3 (Bilan et al., 2013), have relatively low sensitivity and are limited to high-cellular stress experiments such as tail transection. More recently, other redox sensors developed for use in cell-based assays have been applied in zebrafish through transient mRNA injections, but these are neither stable or sensitive for studies applied to assess stressors of environmental or pharmaceutical relevance (Zou et al., 2018). With this in mind, a model that provides the ability to detect imbalances in cellular RedOx status operating through Nrf2, as a master regulator of antioxidant defences across the whole organism, would provide a powerful means by which to quantify the impacts of exposure to oxidative stress-inducing substances and conditions. Moreover, in addition to its use in environmental toxicology, the zebrafish is an important non-mammalian model in biomedical research mainly due its high degree of genetic similarity with humans. Indeed, at least 70% of human genes possess at least one zebrafish ortholog, and 82% of genes involved in human diseases have at least one zebrafish ortholog (Bradford et al., 2017; Howe et al., 2013). Furthermore, the zebrafish genome is sequenced and readily edited through knock-out/knock-in experiments with morpholinos, mRNA, and plasmid injections, or more precisely with the advent of CRISPR-Cas9 gene editing technology (Irion et al., 2014; Lieschke and Currie, 2007; Kari et al., 2007).

Here, we aimed at developing a biosensor zebrafish for OS unrestricted by tissue-specific expression profiles, for the screening of aquatic pollutants and novel biomedical drugs. We hypothesised that by using EpRE as a global marker of cellular responses to OS, we would observe chemical-dependent tissue expression profiles with high detection sensitivity. We tested our model through exposure to five compounds of environmental and/or biomedical relevance, known to exert their toxicity via oxidative mechanisms in specific tissues.

2. Methods

2.1. Fish husbandry and embryo culture

Adult zebrafish were held in flow through aquaria at the University of Exeter, at 28 ± 1 °C, under appropriate conditions for spawning. We used an existing population of Wild Indian Karyotype zebrafish (WIK), maintained as an outcrossed wild type line, to generate transgenic fish and for outbreeding. For transgenic fish generation, eggs were collected at the early 1-cell stage, and for experiments, embryos were held in Petri dishes at 28° ± 1 °C until they were used for drug exposures and subsequent imaging. All embryos were cultured in E3 medium for all our experiments, using a recipe based on that of Kaufman et al. (2009) modified to ensure stable and repeatable carbonate chemistry that could affect the baseline fluorescence expression. Further details of the fish husbandry and culture conditions can be found in the Supplementary Materials and Methods section.

2.2. EpRE-mCherry transgenic lines

The following architecture was used for our construct (Fig. 1): three tandem repeated EpREs (Prestera et al., 1993), combined with an hsp70 minimal promoter (Kimura et al., 2014), mCherry, and polyA sequences, flanked with miniTol2 sequences (Urasaki et al., 2006). We employed three EpRE tandem repeats for enhancing sensitivity. This construct was generated by GeneArt (Thermo Fisher Scientific, California, USA) and placed in a pMX vector. The pMX Tol2-3EpRE-hsp70-mCherry-polyA-Tol2 plasmid was injected (25 ng/μL; 1 nL volume), along with transpose mRNA (25 ng/μL), into early 1-cell stage WIK eggs and the resulting larvae raised to adulthood. These animals constituted the founder adult generation (F_0). F_0 individuals carrying the transgene were identified through out-crossing with WIK fish and eventually three independent stable Tg (*3EpRE:hsp70:mCherry*) lines were established (lines 1, 2 and 3, see Supp Fig. 1). Subsequent experiments were conducted on the F_2 and F_3 generations (see supplementary methods for more information on lineage and screening).

2.3. Induction testing in the three Tg (3EpRE:hsp70:mCherry) lines

To test the ability to induce the *EpRE* construct in stable transgenic individuals, we subjected all three lines developed to a glutathione inhibitor (see Chemical treatment, and Diethylmaleate (DEM) sections) known to induce oxidative stress (Kobayashi et al., 2002; Usenko et al., 2008), and thus representing an appropriate positive control substance. The independent transgenic lines all responded in a similar manner to the global oxidative stress inducer (DEM, Supp Fig. 2). Subsequently, we adopted line 1 as our main experimental line as it presented the lowest level of baseline background activity (Supp Fig. 1) potentially allowing for higher sensitivity for the detection of tissue-specific oxidative stress.

2.4. Chemical treatment

Modified E3 medium (described above), was used to prepare all chemical solutions and the pH was balanced as described above to ensure a pH_{NBS} of 7.0 (± 0.05). To assess the specificity and sensitivity of our transgenic line to oxidative stress, we exposed it to a series of chemicals and a heavy metal known to induce tissue-specific oxidative stress in mammals (Table 1). In all cases, a concentration range was used in order to demonstrate dose responsiveness and to assess model sensitivity. These concentration ranges were designed to encompass a likely range from little/no response to the induction of oxidative stress based upon the prior information from both the literature, and in house data held on uptake and toxicity of these chemicals. These were: diethylmaleate (DEM; Sigma-Aldrich, Dorset, UK); acetaminophen (APAP; Sigma-Aldrich, Dorset, UK); cisplatin (Tocris, Oxford, UK); phenylhydrazine (PhZ; Sigma-Aldrich, Dorset, UK); and Cu^{2+} (dosed as $CuSO_4{\cdot}5H_2O$; Fisher Thermo Scientific, Hemel Hempstead, UK). $CuSO_4{\cdot}5H_2O$ was added directly to the E3 culture medium. All other substances were dissolved in E3 mixed with 0.5% dimethyl sulfoxide (DMSO), which was also used as our vehicle control. Solutions were prepared < 24 h in advance of exposures and kept at 4 °C until just prior to use when they were adjusted to 28 °C. No water changes were conducted during the dosing period (over 48 h, between 2 and 4 dpf).

Healthy 2 dpf larvae were subject to dechorionation with fine forceps (if they had not already hatched; World Precision Instruments cat. #500341) and then exposed for 48 h (from 2 to 4 dpf) individually in 24-well microplates to a range of concentrations of the test substances (see Table 1; one fish per well in 1.2 mL; Corning CoStar 24 well plates, Corning, New York, USA). For Cu^{2+}, which is known to adhere to plastic, fish larvae were exposed in individual glass vials (Fisher Scientific, Hemel Hempstead, UK, cat. #15364769) in a 1.2 mL volume. Following the defined exposure period, larvae were terminated via an overdose of MS-222 (Sigma-Aldrich, Dorset, UK). All experiments were performed three times and each experiment undertaken with a separate batch of embryos, freshly made chemicals, and 5 replicates per treatment concentration (total $n = 15$ for each exposure concentration). Sample size was chosen to balance minimising animal use with statistical rigor for fluorescence detection of compound effects. As such, for each test substance we conducted 3 separate experiments with 5 replicate animals. Imaging duration was optimised for capturing the treatment response while minimising animal stress. Fish larvae were allocated randomly to the treatments, and collected from different batches of parental fish.

2.5. Analytical chemistry

Culture media and larval samples were collected from parallel exposures to assess chemical stability over the exposure period and chemical uptake into exposed larvae (see Supplementary Information).

2.6. Immunohistochemistry for cellular Na^+ K^+ ATPase

Positive identification of cutaneous ionocytes was undertaken by using a mouse anti-Na^+ K^+ ATPase antibody. Detailed methods are provided in the Supplementary materials and methods. All experiments were performed in triplicate ($n = 5$ per treatment, per trial).

2.7. Neuromast staining

To positively identify hair and/or support cells of the neuromasts, live larvae were stained with the nucleic acid stain SYTO24 (ThermoFisher Scientific, Catalog #S7559). Following 48 h exposures to cisplatin, and just prior to imaging, the treatment solutions were removed and replaced with an equal volume of SYTO24 (5 nM in 0.1% DMSO in E3) staining solution for 3 min. Following this, embryos were rinsed (3×) using E3 culture medium prior to embedding and imaging.

2.8. Imaging and image analysis

Full details are contained within the Supplementary Materials and Methods section. Briefly, following exposures larvae were anaesthetised in 0.4 mg/mL MS-222 and mounted in 0.7% low-melting agarose prepared in E3 culture medium also containing 0.4 mg/mL MS-222. Whole-body images of the larvae were obtained on a Zeiss Observer Z1 (Zeiss, Cambridge, UK) with a 10× objective lens, using a brightfield and mCherry filter illuminated with a mercury fluorescent light source. Z-stacks of the entire larvae were taken in segments and the images were processed using a custom focal stacking and stitching framework, “stacknstitch” (Metz, in prep.). Epifluorescence imaging, for whole-body phenotypic characterisation and densitometry was undertaken using a Zeiss Observer Z1 (Zeiss, Cambridge, UK), with a 10× (liver) or

Table 1
Summary of nominal exposure concentrations. All chemicals (except Cu^{2+}) were dissolved in 0.5% DMSO. Animals were housed individually during the study period (2–4 dpf), in 24 well-plates in a volume of 1.2 mL/well.

Compound	Exposure concentrations			
Diethylmaleate	0.5% DMSO	10 μM	20 μM	40 μM
Acetaminophen	0.5% DMSO	1.25 mM	2.5 mM	5 mM
Cisplatin	0.5% DMSO	10 mM	50 mM	100 mM
Phenylhydrazine	0.5% DMSO	0.0125 μM	0.025 μM	0.05 μM
Copper sulfate (II) pentahydrate	E3	1 μg/L	2 μg/L	20 μg/L
Equivalent Cu^{2+}	E3	0.2545 μg/L	0.509 μg/L	5.09 μg/L

20× (kidney) lens, using a bright field and mCherry filter and a mercury fluorescent light source (HXP 120C, Zeiss, Cambridge, UK).

Quantification of mCherry expression was performed using Fiji (imageJ), by tracing around individual organs and measuring pixel intensity in that region. For Cu^{2+}, responding cells were identified by immunohistochemistry (see previous section) and counted in a standardized area on the yolk sac surface (using a set square size on Fiji).

2.9. Statistical analysis

All data were analysed statistically using the PERMANOVA + add in (Anderson et al., 2008) in PRIMER 6.1 (Clarke and Gorley, 2006). As PERMANOVA + is sensitive to differences in dispersion between groups (Anderson, 2006), data were first tested for homogeneity of variance using PERMDISP, a dissimilarity-based extension of Levene's test (Anderson et al., 2008). If data were seen to have heterogeneous variance an appropriate transformation was applied, which varied depending on the level of heterogeneity displayed by groups within each treatment. Euclidean distance similarity matrices were then constructed for all data. To measure the effect of contaminants on fluorescence intensity *p*-values were calculated from 9999 permutations, using an unrestricted permutation of raw data. Pair-wise comparisons were undertaken where a significant main effect was encountered for a factor with more than two levels.

3. Results and discussion

3.1. The 3EpRE:hsp70:mCherry transgenic model

The mechanistic basis of our stable transgenic zebrafish line is summarised in Fig. 1. Three phenotypically-discrete stable F_0 transgenic lines were generated, each displaying a low level expression of mCherry (detected from 2 days post fertilisation, or dpf) in the absence of a stressor (see Supplementary Methods for more details). Of these, the larvae of line 1 showed the lowest level of baseline mCherry expression in untreated animals (Supp Fig. 1A), and consequently this line was used for subsequent chemical exposure experiments. Exposure to DEM, that is known to inhibit glutathione synthesis (our positive control) revealed a wide range of responding tissues consistent with that expected for the oxidative stress-inducing toxicological profile of this chemical. Subsequent exposure to four additional compounds with differing toxicity profiles enable us to show organ-specific and concentration-dependent OS responses consistent with those reported in mammals. Collectively, these data support the functional conservation of the EpRE sequence and the associated Nrf2 signalling pathway in the OS response cascade between mouse and zebrafish (Suzuki et al., 2005; Carvan 3rd et al., 2001; Fuse and Kobayashi, 2017; Kusik et al., 2008). In addition to the expression profiles expected from exposures in mammals, we also identified epidermal, ionoregulatory and vestibule-auditory tissue responses for some compounds, illustrating further the utility of our Tg (*3EpRE:hsp70:mCherry*) zebrafish line for detecting novel OS-related mechanisms. Our stable transgenic zebrafish line provides a significant advancement for detecting organismal responses to Nrf2 activators over previous models where responses have been limited to individual tissues (e.g. olfactory regions (Tsujita et al., 2011)). Our line has shown a stable and inducible fluorescent signal across four generations since its creation. In the longer term, line stability will be ensured by freezing sperm of the Line 1 F4 generation. The line can then be restocked periodically back to the original source thereby avoiding genetic changes through degradation, inbreeding, and/or mutations. Our study used this line as embryo/larvae in order to take advantage of the optical clarity affording organ specific fluorescence visualisation. However, responsiveness of the *3EpRE:hsp70:mCherry* transgene should carry through to adulthood. This raises the possibility of assessing adult responses to oxidative insult which would be achievable through cryo-sectioning/histology and immunohistochemistry using a mCherry antibody. Alternatively, the line could be crossed with pigment deficient mutants such as *casper* (White et al., 2008) or *crystal* (Antinucci and Hindges, 2016), thereby providing optical access to the fluorescent signal in later stages.

3.2. Diethylmaleate (DEM)

Exposure to DEM (Usenko et al., 2008) (at 8.7 μM DEM) revealed elevated mCherry fluorescence in hair cells of the neuromasts and olfactory pits, and also in the fore- and mid-gut. At 17.2 μM DEM, responses also occurred in the pronephric duct, the liver, and the skin. At 35.9 μM DEM, mCherry fluorescence was more pronounced in all of these tissues (Fig. 2D), especially the skin (Fig. 2E). In the liver, fluorescence was concentration-dependent (Supp Fig. 3, Pseudo-$F_3 = 205.35$, $p \leq 0.001$), and was significantly higher for all treatments compared with the corresponding untreated control (0.5% DMSO). Measured concentrations of DEM in the culture medium were close to nominal values but not detected in body tissues (< 0.2 μM limit of quantification; Supp Table 1), indicating low uptake and/or rapid metabolism within the organism. As stated, mCherry fluorescence was not restricted to the olfactory pits, gill, and/or liver, as has been previously reported for Nrf2 specific target genes after exposure to DEM (Nakajima et al., 2011). Our model thus represents an inducible and stable transgenic line that responds as expected to DEM exposure by exhibiting EpRE upregulation across multiple tissues and organs.

3.3. Acetaminophen (APAP)

In mammals, APAP overdose is known to result in both nephrotoxicity and hepatotoxicity mediated by OS. In this response cascade, a highly reactive quinone intermediate metabolite of APAP, *N*-acetyl-p-benzoquinone imine (NAPQI) depletes glutathione and sulfate stores, and binds with cellular proteins causing mitochondrial dysfunction, OS, and DNA damage (Burcham and Harman, 1991; Pumford and Halmes, 1997). Excess NAPQI also triggers increased hepatic infiltration of leukocytes and a range of inflammatory mediators, including ROS, which contribute further to the progression of liver injury (Holt and Ju, 2006; Ishida et al., 2002; Liu et al., 2004). In our *Tg* (*3EpRE:hsp70:mCherry*) fish, APAP treatment resulted in elevated fluorescence primarily in the liver and pronephric proximal tubule, mirroring mammalian target tissues (Fig. 3Di, ii arrowheads). In both organs, the response was concentration-dependent (pronephros:

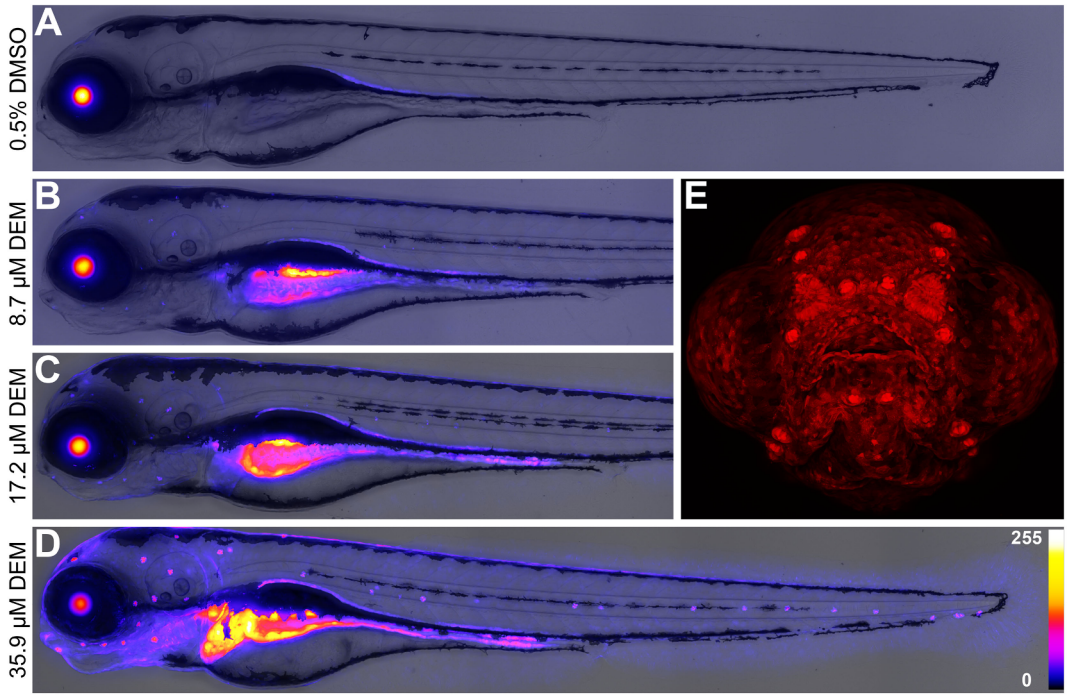

Fig. 2. Concentration-dependent tissue fluorescence in Tg (3EpRE:hsp70:mCherry) zebrafish larvae exposed to diethylmaleate (DEM). Fish larvae were exposed to solvent control (A) and three concentrations of DEM (B; C; D) from 2 to 4 dpf, and subsequently imaged via epifluorescence and confocal microscopy. A confocal image of the frontal head region (E) is presented to illustrate the range of surface tissues (e.g. skin cells, neuromasts, olfactory pits) affected by exposure to 35.9 µM DEM. For images (A–D), fluorescence intensity is represented using a "Fire" lookup table with a 0–255 pixel intensity calibration bar. Measured DEM E3 culture medium concentrations displayed.

Pseudo-F_3 = 27.075, $p \leq 0.001$; liver Pseudo-F_3 = 53.798, $p \leq 0.001$). In the liver, mCherry was significantly higher at all concentrations compared with the DMSO control, and was also significantly different between each treatment (Supp Fig. 3B). For the pronephros, fluorescence was higher for all measured concentrations compared with the DMSO control, but did not significantly differ between 2.2 and 4.5 mM (Supp Fig. 3B). Measured APAP concentrations in culture medium were close to nominal values, and approximately 10% of APAP was absorbed into the larvae when internal and external measured concentrations were compared (Supp Table 1). Our data for APAP indicates a

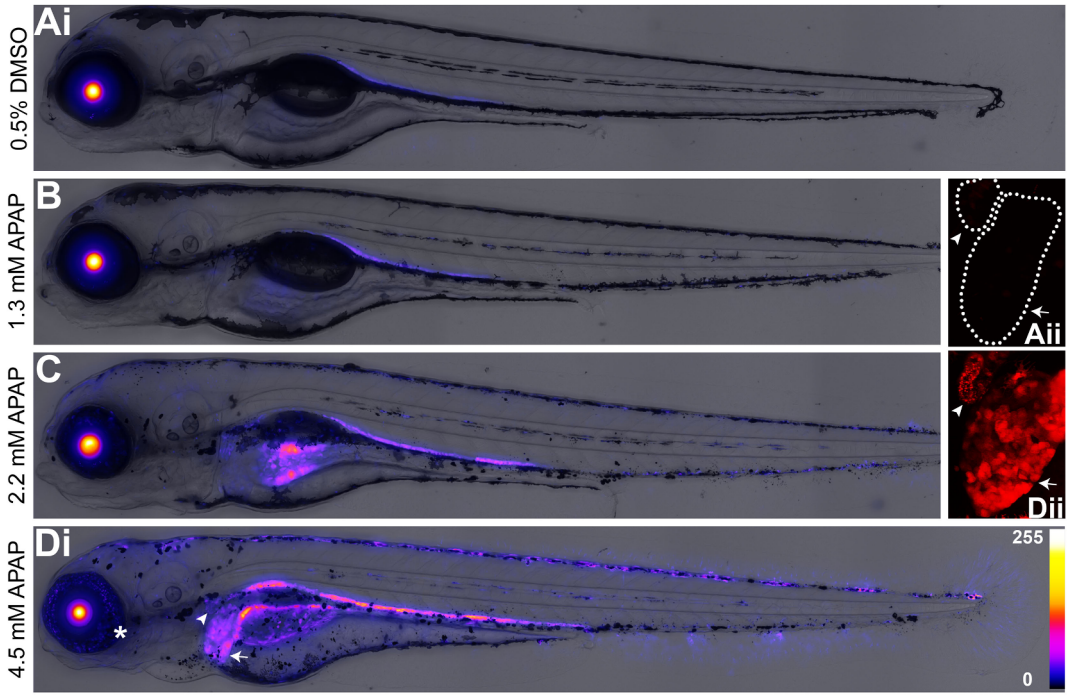

Fig. 3. Concentration-dependent tissue responses in Tg (3EpRE:hsp70:mCherry) zebrafish larvae exposed to acetaminophen (APAP). Fish larvae were exposed to a solvent control (Ai, ii) and three concentrations of APAP (B; C; Di, ii) from 2 to 4 dpf and subsequently imaged via epifluorescence and confocal microscopy. Confocal images illustrate a pronephric convoluted tubule and the liver under control (Aii) and 4.5 mM APAP (Dii) conditions. Arrowheads = pronephric convoluted tubule; arrows = liver; asterisk = retina. For images A–D, fluorescence intensity is represented using a "Fire" lookup table with a 0–255 pixel intensity calibration bar. Measured APAP culture medium concentrations displayed.

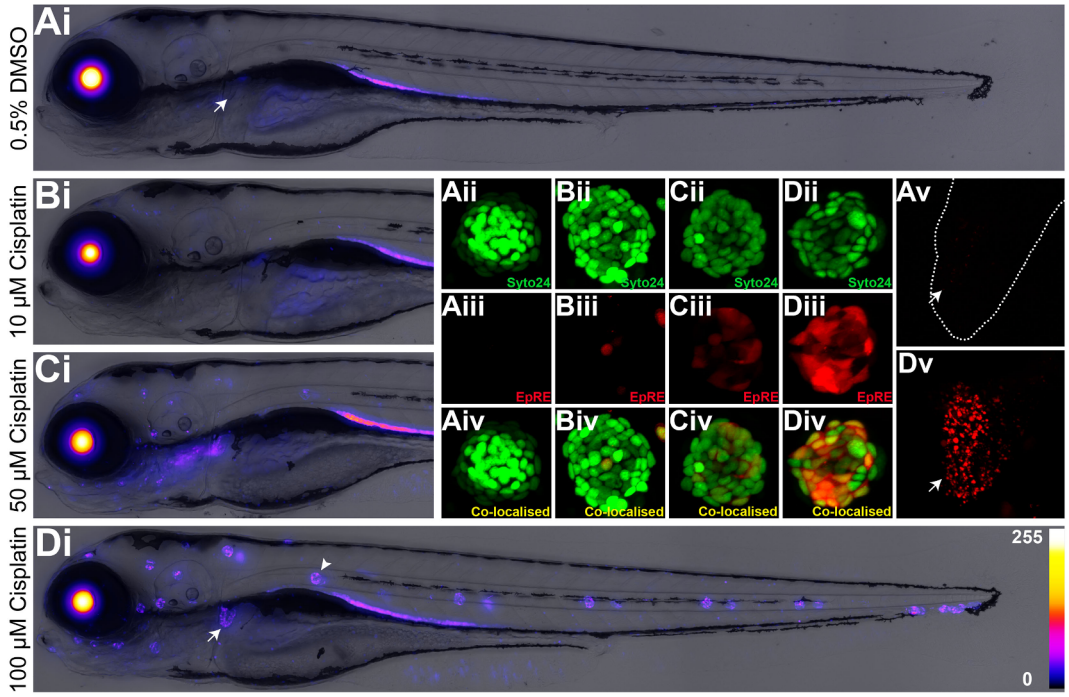

Fig. 4. Concentration-dependent tissue responses in Tg (3EpRE:hsp70:mCherry) zebrafish larvae exposed to cisplatin. Fish larvae were exposed to solvent control (Ai-v) and three concentrations of cisplatin (Bi-v; Ci-v; Di-v) from 2 to 4 dpf and subsequently imaged via epifluorescence and confocal microscopy. Confocal images of a lateral line neuromast labelled with SYTO24 and EpRE-mCherry expression and their colocalization, under control (Aii-v) and cisplatin exposed conditions (Bii-iv, Cii-iv, Dii-iv). Confocal images of a pronephric convoluted tubule under control (Av) and 100 µM cisplatin (Dv) Arrowheads = neuromast; arrow = pronephric convoluted tubule. For images A–D, fluorescence intensity is represented using a "Fire" lookup table with a 0–255 pixel intensity calibration bar. Nominal cisplatin culture medium concentrations displayed.

concentration-dependant alteration of hepatocyte ReDox balance in the zebrafish, and supports the findings of a single study of a glutathione reduction in the zebrafish liver after APAP overdose (North et al., 2010). APAP exposures has previously also been demonstrated to cause renal toxicity in zebrafish (Peng et al., 2010) and here, for the first time, we furthermore provide evidence supporting an oxidative stress-mediated toxicity pathway via activation of the EpRE element in the pronephros.

Aqueous exposures to sub-lethal concentrations of APAP during larval development have been shown to result in a concentration-dependent decrease in pigmentation in retinal cells, the head, and the yolk sac region (David and Pancharatna, 2009). Here we also show this and offer evidence for an oxidative stress-mediated mechanism, as exposure resulted in decreased pigmentation and fluorescence induction in pigment cells including those of the retina (Fig. 3Di asterisk). Interestingly, APAP has been shown, in human epidermal melanocytes *in vitro*, to inhibit melanin biosynthesis in a concentration-dependent manner, by decreasing both melanin content and tyrosinase activity (Wrzesniok et al., 2016).

3.4. Cisplatin

In mammals, nephrotoxicity in response to exposure to the alkylating agent and chemotherapeutic drug cisplatin is a complex multifactorial process thought to arise partly from the activation of several signalling pathways in renal tubular cells including the depletion of cellular glutathione and interference of mitochondrial function (Kruidering et al., 1997). Furthermore, cisplatin is also a well-known ototoxic agent acting via an ROS mediated mechanism, linked to NOX-3 in the cochlea. Cisplatin activates NOX-3, increasing production of superoxide (Banfi et al., 2004) which leads to the depletion of glutathione and a cascade of events ultimately resulting in apoptosis in the cochlea (Lee et al., 2004). Our *Tg* (*3EpRE:hsp70:mCherry*) zebrafish showed a concentration-dependent induction of mCherry in the proximal convoluted tubules of the pronephros in response to cisplatin exposure (Fig. 4Di, v arrow) (Pseudo-F_3 = 22.336, $p \leq 0.001$), with significantly higher fluorescence exhibited after exposure to 50 and 100 µM cisplatin (nominal) compared with the control (Supp Fig. 3C). Cisplatin uptake into the larvae was relatively low (3–4% of the medium) but was nevertheless concentration-dependent (Supp Table 1), aligning with the biological responses seen. The ROS response seen in specific sub regions of the pronephros in our study, therefore, is consistent with the established nephrotoxicity of cisplatin in mammals, and the proximal tubule injury previously reported in the zebrafish (Hentschel et al., 2005).

Mechano-sensory hair cells in neuromasts in the zebrafish, which can be visualised through the use of vital dyes, have been widely used as a surrogate model for ototoxicity (Buck et al., 2012). In a number of published studies, cisplatin has been shown to induce concentration-dependent and time-sensitive lateral line hair cell loss (Buck et al., 2012; Choi et al., 2013; Ou et al., 2007) and here we evidence that hair cell damage in the neuromasts of zebrafish by cisplatin is likely linked to oxidative stress (Fig. 4D arrowhead). Using the nucleic acid stain SYTO24, in combination with confocal co-localisation, we also show that EpRE activation is not restricted to hair cells, but occurs also in the support cells of the neuromasts (Fig. 4A/Dii-iv).

3.5. Phenylhydrazine (PhZ)

In mammals, the haemotoxic mechanism of PhZ is thought to be via the formation of H_2O_2 and its subsequent interaction with erythrocytes. The oxidised form of PhZ can directly denature haemoglobin, and induce the peroxidation of red cell membrane lipids (Clemens et al., 1984). Here we show that *Tg* (*3EpRE:hsp70:mCherry*) zebrafish larvae exposed to PhZ displayed an increase in mCherry fluorescence in circulating erythrocytes (Fig. 5). Confocal microscopy analysis on a standardized segment of the caudal artery shows PhZ had a significant effect on the number of mCherry-expressing erythrocytes (Pseudo-F_3 = 117.35, $p \leq 0.001$). Exposures to 0.025 and 0.05 µg/mL PhZ (nominal), revealed that the % of fluorescent erythrocytes was higher compared to the DMSO control (~20 and ~60%

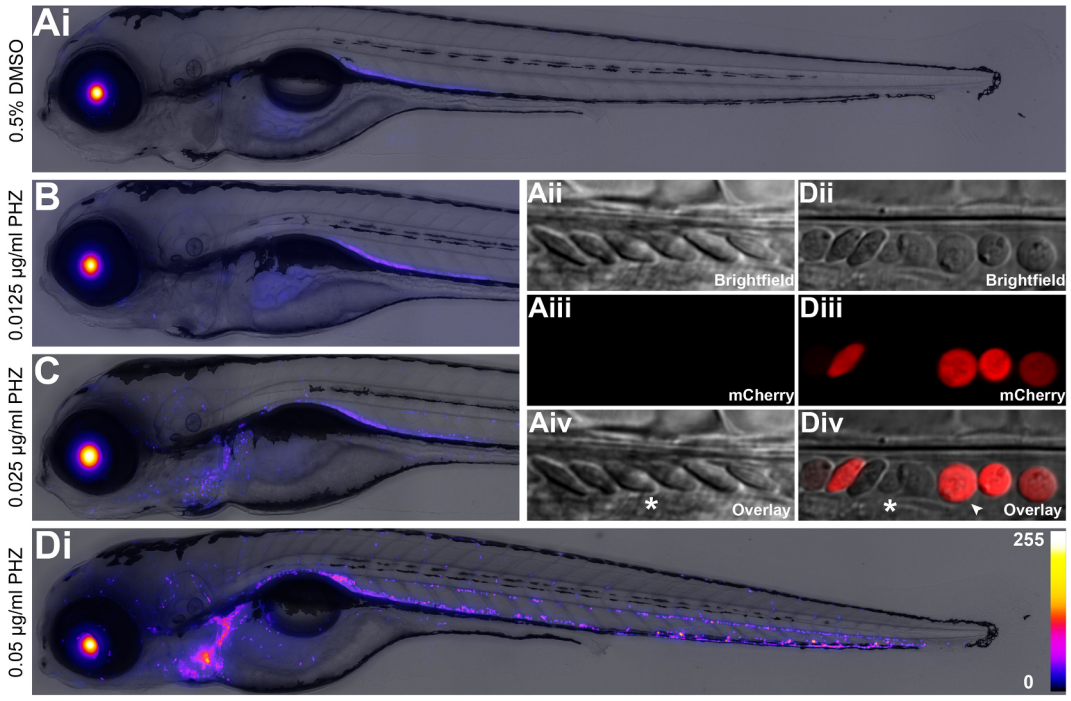

Fig. 5. Concentration-dependent tissue response in Tg (3EpRE:hsp70:mCherry) - zebrafish larvae exposed to phenylhydrazine (PhZ). Larvae were exposed to a solvent control (Ai-iv) and three concentrations of PhZ (B; C; Di-iv) from 2 to 4 dpf and subsequently imaged via epifluorescence and confocal microscopy. Confocal images of a section of the caudal artery under control (Aii-iv) and 0.05 µg/mL PhZ (Dii-iv) conditions. Arrowheads = responsive erythrocytes; asterisk = non-responsive erythrocytes. For images (A–D), fluorescence intensity is represented using a "Fire" lookup table with a 0–255 pixel intensity calibration bar. Nominal PhZ culture medium concentrations displayed.

more, respectively; Supp Fig. 3D). PhZ in the medium was not detected on chromatographs as parent compound, and it is thus probable that the observed haemolytic effect may have been due to a degradation product rather than PhZ itself (Supp Table 1). The observation of EpRE-activation in some, but not all, erythrocytes may reflect the presence of different sub-populations of cells (Fig. 5Div). In vertebrate embryos during early life, haematopoiesis occurs in a series of successive waves, and in zebrafish initiation of hematopoietic activity in tissues occurs at different developmental time

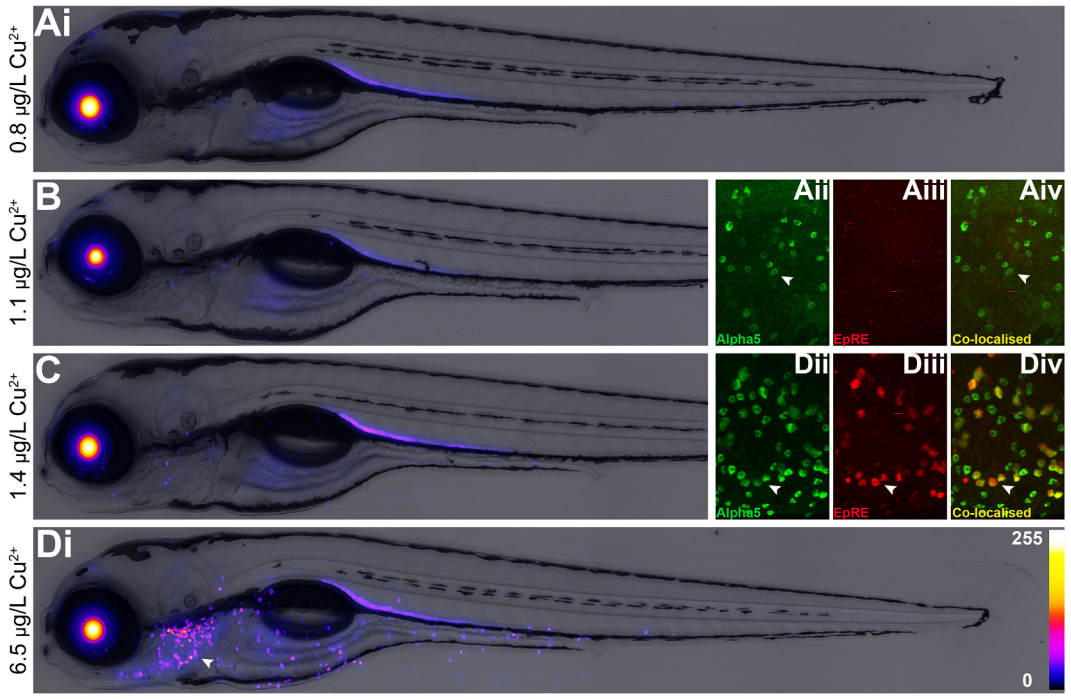

Fig. 6. Concentration-dependent tissue response in Tg (3EpRE:hsp70:mCherry) - zebrafish larvae exposed to Cu^{2+}. Fish larvae were exposed to either a control (0.83 µg/L Cu^{2+}; Ai-iv) or three concentrations of Cu^{2+} (B; C; Di-iv) from 2 to 4 dpf and subsequently imaged via epifluorescence and confocal microscopy. Confocal microscopic images of fixed larvae under control (Aii-iv) and 6.46 µg/L Cu^{2+} (Dii-iv) conditions; green fluorescence indicates staining with an anti-Na^+ K^+ ATPase antibody (alpha5), red fluorescence is EpRE-mCherry signal, and yellow indicates co-localised signal. Arrowheads = ionocytes. For images (A–D), fluorescence intensity is represented using a "Fire" lookup table with a 0–255 pixel intensity calibration bar. Measured Cu^{2+} culture medium concentrations displayed. (For interpretation of the references to color in this figure legend, the reader is referred to the web version of this article.)

points (Davidson and Zon, 2004). Our PhZ exposure window spanned over two days and therefore it is possible that the mosaic expression pattern observed reflects differences in sensitivity to PhZ (or its degradation products) in erythrocytes at different cell developmental stages.

3.6. Copper

Oxidative stress in fish is known to occur following both waterborne and dietary exposures to the important environmental contaminant copper (Cu^{2+}) (Lushchak, 2011). The mechanism of Cu^{2+} toxicity involves ROS production that results from interference with metal-transport and sequestration processes, as well as by directly generating free radicals through valence changes (Lushchak, 2011; Craig et al., 2007). Under homeostasis, ROS damage by transition metal ions is normally prevented by antioxidants including metallothioneins and ferritin (Lushchak, 2011). Our model appears highly sensitive to the induction of EpRE by Cu^{2+} (dosed as $CuSO_4{\cdot}5H_2O$). We were able to detect a measurable mCherry fluorescence response for exposure concentrations as low as 1.1 μg/L Cu^{2+}, which is well within the range of Cu^{2+} in natural freshwaters (e.g. freshwater Cu^{2+} concentrations range between 0.2 and 30 μg/L Cu^{2+}, and upwards for Cu^{2+}-polluted systems (Craig et al., 2007; Hem, 1985; Robins et al., 1997)). Our sensitivity level for detecting OS responses to Cu^{2+} is more than one order of magnitude higher than that reported previously for zebrafish embryos or in adult livers measuring upregulation of OS associated genes (e.g. catalase, superoxide dismutase 1, or gstp1) via RT-QPCR (Craig et al., 2007; Fitzgerald et al., 2016).

EpRE-activation in our model following Cu^{2+} exposure occurred in epithelial cells, especially below the otic vesicle, adjacent to the gill, and in close proximity to the yolk sac (Fig. 6Di arrowhead). In freshwater, teleosts maintain ionic homeostasis using a number of strategies, including the use of specialised osmoregulatory cells, known as ionocytes, which can actively uptake Na^+, Cl^-, and Ca^{2+} and excrete H^+ and HCO_3^- ions (Dymowska et al., 2012). In larval zebrafish, this is achieved predominantly through cutaneous ionocytes (Hwang and Chou, 2013). To establish whether EpRE induction in zebrafish was localised within cutaneous ionocytes, these cells were fluorescently labelled using a mouse anti-Na^+ K^+ ATPase antibody and confocal microscope images were taken to quantify the number of antibody-stained ionocytes (green), ionocytes expressing EpRE (red), and cells with a co-localised signal (yellow), under control (Fig. 6Aii-iv) and 6.46 μg/L Cu^{2+} exposure conditions (Fig. 6Dii-iv). Exposure to Cu^{2+} resulted in a significant increase in the number of ionocytes in exposed larvae compared to control animals (Pseudo-$F_1 = 21.725, p \leq 0.001$), with 64% of these exposed ionocytes also expressing EpRE-mCherry signal (Supp Fig. 3E). This increase in ionocytes may function as a mechanism to counter the blocking effect of Cu^{2+} on Na^{2+}channels in the existing ionocytes, while the mCherry signal suggests these cells are undergoing oxidative stress.

Measured concentrations of Cu^{2+} in the medium were within 10% of nominal values (Supp Table 1). Internal whole-body concentrations of Cu^{2+} were low, and although there was a tendency towards higher concentrations in the Cu^{2+} treated groups compared with controls (Supp Table 1), there were no significant differences. Microscopic analysis supported the analytical chemistry with induction of EpRE signal restricted to the skin surface (Fig. 6), and with no observable effect in the liver or any other internal organs despite previous reports of liver toxicity in adult zebrafish (Craig et al., 2007). Moreover, no oxidative stress occurred in the lateral line hair cells, despite being previous reports suggesting sensitivity to Cu^{2+} (Buck et al., 2012), albeit at a higher exposure level ($IC_{50} \sim 0.5$ μM Cu^{2+} compared to our maximum dosing of 0.1 μM Cu^{2+}).

4. Conclusions

Here, we have developed a novel stable transgenic zebrafish using EpRE as a global marker of cellular responses to oxidative stress, thus avoiding the tissue-restricted profiles of previous Nrf2-focussed lines. Using this model we show tissue-specific and concentration-dependent responses to five compounds well-known to induce oxidative stress and reveal phenotypes comparable with those reported in mammals, thus supporting system and model suitability for both environmental and human health applications. Our fish enables, for the first time, monitoring if, when, and where, a chemical or condition results in cellular RedOx imbalance, and consequently, affords a new, powerful approach for further understanding a wide range of human health and environmental conditions in which oxidative stress is a critical contributing factor. Furthermore, by using our model and construct design, analyses could be conducted on the crosstalk between redox sensitive transcription factors and their interactive roles in pathologies, thereby furthering our understanding of the signalling pathways driving OS (Buelna-Chontal and Zazueta, 2013).

Our approach has potentially broad reaching and diverse applications from the biomonitoring of aquatic environments, to the delineation of toxicity mechanisms associated with the induction of ROS and subsequent signalling cascades in a range of important human diseases. The exposure route used in the current study was via immersion (that likely confers a combination of transdermal, transbranchial and oral uptake), which is of direct relevance to environmental toxicity studies. Importantly, to allow full interpretation of exposure-response relationships, particularly in relation to increasing model relevance for biomedical application, we undertook internal concentration measurements of each chemical. This is a critical aspect often overlooked in biomedical applications of the zebrafish model, yet is vital for interpreting the absence of an effect as a negative result, and for establishing actual effect levels attributable to observed biological changes. Furthermore, in comparison to previous approaches used for assessing oxidative stress, such as measuring antioxidant defence responses (e, g. superoxide dismutase, glutathione etc.), or indicators of oxidative perturbation (e.g. lipid peroxidation, oxidative-DNA damage etc.), our model crucially provides an *in vivo* readout, with tissue/cell-level precision thus providing an early warning (potentially pre oxidative injury) assessment system that also takes into account crucial aspects, such as metabolic activation and oxidative stress-induced signalling cascades, that may otherwise not be recapitulated in cell based assays.

By working with non-protected life stages of zebrafish larvae, our model is furthermore amenable to high throughput screening of chemicals, and may thus contribute to the avoidance of unnecessary animal testing, thereby supporting the principles of reduction, refinement, replacement in animal testing. Indeed, the EpRE transgenic zebrafish embryos provide a unique screening platform, as the inherent advantages of this species coupled with technological advances in microscopy provide the potential for large-scale semi-automated imaging experimental designs. The higher-throughput amenity of our model offers the means for screening new chemicals (including human drugs) for their potential to induce organ-specific oxidative stress, or for their anti-oxidant activity, as well as testing therapies and approaches designed to alleviate the adverse effects of such unwanted cellular processes.

Author contributions

CRT, TK, and SM conceived the project, developed the overall concept, and designed the studies. SM and TK designed the transgenic vector. SM produced the EpRE transgenic zebrafish and undertook the exposure studies and imaging with input from AT and MJW. JAF assisted with all chemical exposures. RPE helped with developing stable water chemistry and exposure conditions, and with the statistical analysis. JM developed the imaging processing pipeline for focal stacking and panorama stitching. CSP performed the copper immunohistochemistry. MT performed the analytical chemistry for diethylmaleate, acetaminophen, and phenylhydrazine. SM, MJW, and CRT wrote the manuscript with input from TK.

Declaration of competing interest

The authors declare that they have no known competing financial interests or personal relationships that could have appeared to influence the work reported in this paper.

Acknowledgements

This work was funded by the UK Natural Environmental Research Council (NE/L007371/1) on a grant to CRT and TK and by a European Union Horizon 2020 research and innovation programme grant - **P**hysiologically **A**nchored **T**ools for **R**ealistic nan**O**materia**L** hazard a**S**sessment (PATROLS) to CRT. We thank members of the Aquatic Resources Centre for their support in maintaining and breeding the fish.

Appendix A. Supplementary data

Supplementary data to this article can be found online at https://doi.org/10.1016/j.envint.2019.105138.

References

Anderson, M., 2006. Distance-based tests for homogeneity of multivariate dispersions. Biometrics 62 (1), 245–253.
Anderson, M.J., Gorley, R.N., Clarke, K.R., 2008. PERMANOVA + for Primer: Guide to Software and Statistical Methods. PRIMER-E, Plymouth.
Antinucci, P., Hindges, R., 2016. A crystal-clear zebrafish for in vivo imaging. Sci. Rep. 6, 29490.
Banfi, B., et al., 2004. NOX3, a superoxide-generating NADPH oxidase of the inner ear. J. Biol. Chem. 279 (44), 46065–46072.
Bilan, D.S., et al., 2013. HyPer-3: a genetically encoded H(2)O(2) probe with improved performance for ratiometric and fluorescence lifetime imaging. ACS Chem. Biol. 8 (3), 535–542.
Bradford, Y.M., et al., 2017. Zebrafish models of human disease: gaining insight into human disease at ZFIN. ILAR J. 58 (1), 4–16.
Buck, L.M., Winter, M.J., Redfern, W.S., Whitfield, T.T., 2012. Ototoxin-induced cellular damage in neuromasts disrupts lateral line function in larval zebrafish. Hear. Res. 284 (1–2), 67–81.
Buelna-Chontal, M., Zazueta, C., 2013. Redox activation of Nrf2 & NF-kappaB: a double end sword? Cell. Signal. 25 (12), 2548–2557.
Burcham, P.C., Harman, A.W., 1991. Acetaminophen toxicity results in site-specific mitochondrial damage in isolated mouse hepatocytes. J. Biol. Chem. 266 (8), 5049–5054.
Burhans, W.C., Heintz, N.H., 2009. The cell cycle is a redox cycle: linking phase-specific targets to cell fate. Free Radic. Biol. Med. 47 (9), 1282–1293.
Carvan 3rd, M.J., et al., 2001. Oxidative stress in zebrafish cells: potential utility of transgenic zebrafish as a deployable sentinel for site hazard ranking. Sci. Total Environ. 274 (1–3), 183–196.
Choi, J., et al., 2013. Protective effects of apocynin on cisplatin-induced ototoxicity in an auditory cell line and in zebrafish. J. Appl. Toxicol. 33 (2), 125–133.
Clarke, K.R., Gorley, R.N., 2006. Primer v6: User Manual/Tutorial. PRIMER-E, Plymouth.
Clemens, M.R., Remmer, H., Waller, H.D., 1984. Phenylhydrazine-induced lipid peroxidation of red blood cells in vitro and in vivo: monitoring by the production of volatile hydrocarbons. Biochem. Pharmacol. 33 (11), 1715–1718.
Craig, P.M., Wood, C.M., McClelland, G.B., 2007. Oxidative stress response and gene expression with acute copper exposure in zebrafish (Danio rerio). Am. J. Physiol. Regul. Integr. Comp. Physiol. 293 (5), R1882–R1892.
David, A., Pancharatna, K., 2009. Effects of acetaminophen (paracetamol) in the embryonic development of zebrafish, Danio rerio. J. Appl. Toxicol. 29 (7), 597–602.
Davidson, A.J., Zon, L.I., 2004. The 'definitive' (and 'primitive') guide to zebrafish hematopoiesis. Oncogene 23 (43), 7233–7246.
Dymowska, A.K., Hwang, P.P., Goss, G.G., 2012. Structure and function of ionocytes in the freshwater fish gill. Respir. Physiol. Neurobiol. 184 (3), 282–292.
Faria, A., Persaud, S.J., 2017. Cardiac oxidative stress in diabetes: mechanisms and therapeutic potential. Pharmacol. Ther. 172, 50–62.
Fitzgerald, J.A., et al., 2016. Hypoxia suppressed copper toxicity during early development in zebrafish embryos in a process mediated by the activation of the HIF signaling pathway. Environ. Sci. Technol. 50 (8), 4502–4512.
Forman, H.J., Torres, M., 2002. Reactive oxygen species and cell signaling. Am. J. Respir. Crit. Care Med. 166, S4–S8.
Freeman, B.A., Crapo, J.D., 1982. Biology of disease: free radicals and tissue injury. Laboratory Investigation; A Journal of Technical Methods and Pathology 47 (5), 412–426.
Fuse, Y., Kobayashi, M., Molecules 2017, 22(3), 436;, 2017. Conservation of the Keap1-Nrf2 system: an evolutionary journey through stressful space and time. Molecules 22 (3), 436.
Hem, J.D., 1985. Study and Interpretation of the Chemical Characteristics of Natural Water. 3rd ed., US Geological Survey Water-Supply Paper 2254. University of Virginia, Charlottesville.
Hentschel, D.M., et al., 2005. Acute renal failure in zebrafish: a novel system to study a complex disease. Am. J. Physiol. Renal Physiol. 288 (5), F923–F929.
Holt, M.P., Ju, C., 2006. Mechanisms of drug-induced liver injury. AAPS J. 8 (1), E48–E54.
Howe, D.G., et al., 2013. ZFIN, the zebrafish model organism database: increased support for mutants and transgenics. Nucleic Acids Res. 41 (Database issue), D854–D860.
Hwang, P.-P., Chou, M.-Y., 2013. Zebrafish as an animal model to study ion homeostasis. Pflugers Arch 465 (9), 1233–1247.
Irion, U., Krauss, J., Nusslein-Volhard, C., 2014. Precise and efficient genome editing in zebrafish using the CRISPR/Cas9 system. Development 141 (24), 4827–4830.
Ishida, Y., et al., 2002. A pivotal involvement of IFN-gamma in the pathogenesis of acetaminophen-induced acute liver injury. FASEB J. 16 (10), 1227–1236.
Itoh, K., Mimura, J., Yamamoto, M., 2010. Discovery of the negative regulator of Nrf2, Keap1: a historical overview. Antioxid. Redox Signal. 13 (11), 1665–1678.
Kari, G., Rodeck, U., Dicker, A.P., 2007. Zebrafish: an emerging model system for human disease and drug discovery. Clin. Pharmacol. Ther. 82 (1), 70–80.
Kaufman, C.K., White, R.M., Zon, L., 2009. Chemical genetic screening in the zebrafish embryo. Nat. Protoc. 4 (10), 1422–1432.
Kehrer, J.P., Klotz, L.O., 2015. Free radicals and related reactive species as mediators of tissue injury and disease: implications for health. Crit. Rev. Toxicol. 45 (9), 765–798.
Kimura, Y., Hisano, Y., Kawahara, A., Higashijima, S., 2014. Efficient generation of knock-in transgenic zebrafish carrying reporter/driver genes by CRISPR/Cas9-mediated genome engineering. Sci. Rep. 4, 6545.
Kobayashi, M., et al., 2002. Identification of the interactive interface and phylogenic conservation of the Nrf2-Keap1 system. Genes Cells 7 (8), 807–820.
Kobayashi, M., Yamamoto, M., 2006. Nrf2-Keap1 regulation of cellular defense mechanisms against electrophiles and reactive oxygen species. Adv. Enzym. Regul. 46, 113–140.
Kruidering, M., Van de Water, B., de Heer, E., Mulder, G.J., Nagelkerke, J.F., 1997. Cisplatin-induced nephrotoxicity in porcine proximal tubular cells: mitochondrial dysfunction by inhibition of complexes I to IV of the respiratory chain. J. Pharmacol. Exp. Ther. 280 (2), 638–649.
Kusik, B.W., Carvan 3rd, M.J., Udvadia, A.J., 2008. Detection of mercury in aquatic environments using EPRE reporter zebrafish. Marine biotechnology (New York, N.Y.) 10 (6), 750–757.
Lee, J.E., et al., 2004. Role of reactive radicals in degeneration of the auditory system of mice following cisplatin treatment. Acta Otolaryngol. 124 (10), 1131–1135.
Lieschke, G.J., Currie, P.D., 2007. Animal models of human disease: zebrafish swim into view. Nat. Rev. Genet. 8 (5), 353–367.
Liska, D.J., 1998. The detoxification enzyme systems. Altern. Med. Rev. 3 (3), 187–198.
Liu, Z.X., Govindarajan, S., Kaplowitz, N., 2004. Innate immune system plays a critical role in determining the progression and severity of acetaminophen hepatotoxicity. Gastroenterology 127 (6), 1760–1774.
Lushchak, V.I., 2011. Environmentally induced oxidative stress in aquatic animals. Aquat. Toxicol. 101 (1), 13–30.
Maritim, A.C., Sanders, R.A., Watkins, J.B., 2003. Diabetes, oxidative stress, and antioxidants: a review. J. Biochem. Mol. Toxicol. 17 (1), 24–38.
Menegon, S., Columbano, A., Giordano, S., 2016. The dual roles of NRF2 in cancer. Trends Mol. Med. 22 (7), 578–593.
Metz J (stacknstitch: An Automated Image Focal-Stacking and Stitching Framework in Python. In preparation.
Nakajima, H., et al., 2011. Tissue-restricted expression of Nrf2 and its target genes in zebrafish with gene-specific variations in the induction profiles. PLoS One 6 (10), e26884.
North, T.E., et al., 2010. PGE2-regulated wnt signaling and N-acetylcysteine are synergistically hepatoprotective in zebrafish acetaminophen injury. Proc. Natl. Acad. Sci. U. S. A. 107 (40), 17315–17320.
Ou, H.C., Raible, D.W., Rubel, E.W., 2007. Cisplatin induced hair cell loss in zebrafish (Danio rerio) lateral line. Hear. Res. 233 (1–2), 46–53.
Peng, H.C., et al., 2010. Nephrotoxicity assessments of acetaminophen during zebrafish embryogenesis. Comp. Biochem. Physiol. C. Toxicol. Pharmacol. 151 (4), 480–486.
Poprac, P., et al., 2017. Targeting free radicals in oxidative stress-related human diseases. Trends Pharmacol. Sci. 38 (7), 592–607.
Prestera, T., Holtzclaw, W.D., Zhang, Y., Talalay, P., 1993. Chemical and molecular regulation of enzymes that detoxify carcinogens. Proc. Natl. Acad. Sci. U. S. A. 90 (7), 2965–2969.
Pumford, N.R., Halmes, N.C., 1997. Protein targets of xenobiotic reactive intermediates. Annu. Rev. Pharmacol. Toxicol. 37, 91–117.
Ray, P.D., Huang, B.W., Tsuji, Y., 2012. Reactive oxygen species (ROS) homeostasis and redox regulation in cellular signaling. Cell. Signal. 24 (5), 981–990.
Robins, R.G., et al., 1997. Chemical, Physical and Biological Interaction at the Berkeley Pit, Butte, Montana. pp. 529–541.
Suzuki, T., et al., 2005. Pi class glutathione S-transferase genes are regulated by Nrf 2 through an evolutionarily conserved regulatory element in zebrafish. Biochem. J. 388 (Pt 1), 65–73.
Tsujita, T., et al., 2011. Nitro-fatty acids and cyclopentenone prostaglandins share strategies to activate the Keap1-Nrf2 system: a study using green fluorescent protein transgenic zebrafish. Genes Cells 16 (1), 46–57.
Urasaki, A., Morvan, G., Kawakami, K., 2006. Functional dissection of the Tol2 transposable element identified the minimal cis-sequence and a highly repetitive sequence in the subterminal region essential for transposition. Genetics 174 (2), 639–649.
Usenko, C.Y., Harper, S.L., Tanguay, R.L., 2008. Fullerene C(60) exposure elicits an oxidative stress response in embryonic zebrafish. Toxicol. Appl. Pharmacol. 229 (1), 44–55.
White, R.M., et al., 2008. Transparent adult zebrafish as a tool for in vivo transplantation analysis. Cell Stem Cell 2 (2), 183–189.
Wiegman, C.H., et al., 2015. Oxidative stress–induced mitochondrial dysfunction drives inflammation and airway smooth muscle remodeling in patients with chronic obstructive pulmonary disease. J. Allergy Clin. Immunol. 136 (3), 769–780.
Wrzesniok, D., et al., 2016. Effect of paracetamol on melanization process in human epidermal melanocytes. Acta Pol. Pharm. 73 (3), 653–658.
Zou, Y., Wang, A., Shi, M., Chen, X., Liu, R., Li, T., et al., 2018. Analysis of redox landscapes and dynamics in living cells and in vivo using genetically encoded fluorescent sensors. Nat. Protoc. 13, 2362–2386.